COMMUNICATION

ChemComm
www.rsc.org/chemcomm

Kinetic isotope effects on the dissolution kinetics of solid salicylic acid in aqueous solution: evidence for solubilisation *via* a proton dissociation–recombination mechanism†

Shelley J. Wilkins, Barry A. Coles and Richard G. Compton*

Physical and Theoretical Chemistry Laboratory, Oxford University, South Parks Road, Oxford, UK OX1 3QZ. E-mail: richard.compton@chemistry.ox.ac.uk

Received (in Cambridge, UK) 21st December 2001, Accepted 18th February 2002
First published as an Advance Article on the web 5th March 2002

Quantitative Atomic Force Microscopy measurements made on the dissolving surface of solid salicylic acid in H_2O and D_2O reveal a kinetic isotope effect ($k_H/k_D = 2.3 \pm 0.6$) on the dissolution rate consistent with a transition state in which the proton is dissociated from the dissolving molecule.

Understanding the chemistry at insulator–liquid interfaces is of great general importance for a huge range of processes from drug dissolution through reactive dyeing to geological weathering.[1] Nevertheless in comparison with other interfaces, such as the gas–solid interface, little kinetic and mechanistic information has been available, partly because of the difficulties extracting kinetic data, even for comparatively 'simple' processes such as dissolution. The recent development in this context of scanned probe methods such as SECM[2] and AFM[3] has to a significant extent overcome these limitations and we have recently used AFM measurements under defined hydrodynamic conditions[4,5] to establish the kinetic rate loss for the dissolution of, for example, calcium carbonate[5] and salicylic acid.[6] For these purposes a novel flow cell was developed, based on the Topometrix[7] liquid immersion cell, with the addition of an inlet tube shaped to allow a jet of fluid to be applied directly to the sample surface, flowing along the front of the cantilever support chip and over the cantilever. The rate of interfacial reaction is measured directly by averaging the absolute height of the imaged surface as indicated by the z-piezo voltage and by following the changes of the height from successive scans. The flow pattern in the cell is complex but has been solved in three-dimensions using a finite-element fluid dynamics program.[8] Knowledge of the flow pattern allows the modelling of convective-diffusion processes within the cell and hence the rigorous determination of interfacial rate laws in terms of the pertinent concentrations local to the solid surface.

In the case of salicylic acid (HSA), the dissolution in water has been studied as a function of flow rate and quantitatively interpreted using a model combining dissolution with the partial re-precipitation, the latter having a first-order dependence on the surface concentration $[HSA]_0$. The net dissolution flux is J/mol cm^{-2} s^{-1} = $k_f - k_b[HSA]_0$ where k_f and k_b and are the rate constants for the dissolution and precipitation respectively. In the modelling the ratio k_f/k_b was constrained to be equal to the measured solubility of HSA. This simple equation was found to give a good fit to the kinetic data obtained in pure water and also in the presence of LiCl, NaCl and $MgCl_2$ (at levels up to 1 M) where the solubility of HSA is significantly reduced.[6,9]

The study of kinetic isotope effects has considerably illuminated the mechanistic study of homogeneous chemical reactions.[10] Accordingly and to the best of our knowledge, entirely novelly, in the context of solubilisation kinetics, we have studied and compared the dissolution of HSA into H_2O and D_2O. Salicylic acid crystals of 0.5–8 mm were grown over 200 h from a saturated solution in ethanol by gradually decreasing the temperature from 30 to 25 °C. Salicylic acid crystals were indexed using standard methods with a NONIUS KCCD diffractometer using MoKα radiation (λ = 0.71073 A). In our experiments, X-ray diffraction analysis revealed that the salicylic acid crystals were monoclinic with space group $P2_1/a$ with a = 11.43, b = 11.19 and c = 4.91 Å. These are in good agreement with published values[11]. A Topometrix TMX 2010 atomic force microscope operating in contact mode with SFM probes type 1520-00 and a 75 μm scanner type 5590-00 was used to obtain the images. The hydrodynamic flow cell used for *in-situ* AFM imaging has been described in detail elsewhere.[4,5]

For dissolution measurements, a crystal of salicylic acid typically 3 × 1 × 1 mm in size exposing the 110 face was mounted on a latex substrate. A new crystal was used for each experiment. The latex mount was sealed inside the flow cell and solution passed through at rates ranging from 2.5 to 17.4 μL s^{-1}. The crystals were allowed to equilibrate in the solvent environment by flowing the solution over the crystal for 20 min before recording image sequences. Images of area 20 × 20 μm were recorded in a continuous sequence at approximately 60 s intervals at each of the flow rates. The average piezo voltage was calculated for each scan and hence the change in height of the mean surface level was derived using the calibration factor of 0.333 V μm^{-1} determined for the scanner. The flow system was gravity fed from a reservoir; the flow rates were varied by adjusting the height difference between the reservoir and capillary outlet. Measurements were taken at a temperature of 21 °C.

The total solubilities of HSA at 21 °C were determined in both H_2O and D_2O by UV spectrophotometric analysis. An excess of HSA was added to 10 mL flasks of either D_2O (70%) or H_2O and left to equilibrate for 24 h. A small aliquot was removed from each of the flasks and centrifuged to separate the excess HSA from the saturated solution. The solutions were diluted 100-fold with phosphate buffer of pH 7.43 and the solubility calculated from the UV absorption spectra. The values found were 14.4 mM (D_2O) and 16.5 mM (H_2O).

Modelling of the kinetic data was performed using FIDAP, a fluid dynamics program which employs finite element methods to solve flow cell problems. A three-dimensional flow simulation of the cell has been described fully previously.[6] The flow region is divided into elements connected together at nodes, appropriate boundary conditions are applied based on the boundaries and surfaces exposed in the flow cell. The equations of momentum, mass and energy are solved for each element and the values for velocities, pressure, temperature and concentrations at each node are obtained. In this simulation data files were prepared containing x, y and z components of velocity at 35 769 points in the smaller volume starting at the mouth of the jet and enclosing the scanning cantilevers, for 14 flow rates encompassing the practical range of the cell. These data files may be freely downloaded from the world wide web.[12] The grid files can be adjusted for temperature and fluid variations by use of the Reynolds number:

$$v_f = (\mathrm{Re} \times d \times \eta)/\rho$$

† Electronic supplementary information (ESI) available: plot of dissolution *vs*. flow rate for the dissolution of the (110) face of salicylic acid in water and D_2O. Links to refs. 12 and 15. See http://www.rsc.org/suppdata/cc/b1/b111642h/

DOI: 10.1039/b111642h

where $v_f$is the flow rate, Re is the Reynolds number, d is the hydraulic diameter of the jet at 0.054 cm, η is the absolute viscosity and ρ is the fluid density. The viscosity and density values used in our simulations for each of the solutions were calculated from published data as shown in Table 1.

Table 1 Viscosity and density data for H_2O and D_2O

Species	Viscosity/cP	Density/g cm^{-3}	Ref.
H_2O	0.9779	0.998	13
D_2O	0.9219	1.075	14

Simulations of chemical processes within the cell were carried out by finite difference methods in two-dimensions as described fully elsewhere.[6] Two FORTRAN 77 programs were prepared. The first of these finds the solution flow path which passes over the scanning tip position and generates a 2D grid file of velocities in a surface which follows the flow path. The second program performs a bicubic spline interpolation from this 2D grid to provide the velocity components in a user specified grid, further details of which may be obtained from our web page.[15] A value of 7.1×10^{-6} cm^2 s^{-1} was used for the diffusion coefficient of HSA in H_2O; in D_2O this was adjusted to 7.5×10^{-6} cm^2 s^{-1} assuming the Einstein–Stokes relation.

The crystal structure of salicylic acid is monoclinic with four molecules contained within the unit cell with dimeric units close to the surface as shown in Fig. 1. The slowest growing and hence the largest surface is the (110) face thus easily distinguishable for imaging purposes.

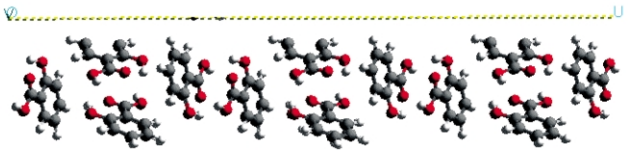

Fig. 1 Crystal structure of SA showing the (110) plane.

Images of the (110) surface *ex-situ* prior to dissolution experiments typically showed the surface to be flat with a few minor defects. Incomplete layers on the surface resulted in macrosteps typically no more than 100 nm in height. The morphology of the (110) plane exposed to water has been described previously.[5,6] The surface is very rough with hillocks and large macrosteps typically 3 μm high. The rate constant $k_f^H$for the dissolution of the (110) face in water in these experiments was found to be 2.0×10^{-8} mol cm^{-2} s^{-1}, at 21 °C, with solubility (k_f^H/k_b^H) of 16.5 mM. This single parameter was capable of quantifying the net dissolution rates across the full range of flow rates studied in pure water.

In D_2O a similar morphology was observed, as shown in Fig. 2. Again, a single rate constant $k_f^D = 8.85 \times 10^{-9}$ mol cm^{-2} s^{-1}, with a solubility (k_f^D/k_b^D) of 14.4 mM was found to describe the kinetic data over the entire flow rate range studied. Consideration of the above kinetic data reveals a significant isotope effect of $k_f^H/k_f^D = 2.3 \pm 0.6$. We suggest that the high value of this ratio is not incompatible with a dissolution mechanism in which the HSA is dissociated in the transition state. It is well known[10] that weak acids, LA, are always weaker in heavy water than in light water. Thus for the reaction:

$$LA(aq) + L_2O \rightleftharpoons L_3O^+ + A^-(aq)$$

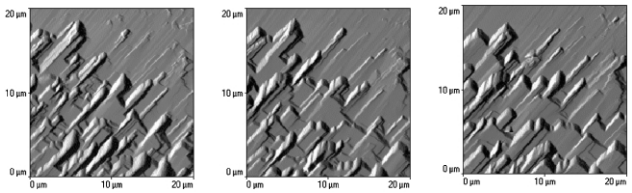

Fig. 2 *In-situ* AFM images of the (110) surface of salicylic acid during the dissolution process in D_2O flowing at a rate of 0.012 cm^3 s^{-1}. Sequence after (left) 0, (middle) 51, and (right) 102 s.

the ratio of acid dissociation constants, $K_A^H/K_A^D \approx 3.0$. This has been understood in terms of fractionation theory[10] or alternatively semi-quantitatively[16] by noting that the stretching vibrations of the H_3O^+ ions have a considerably lower frequency (2900 cm^{-1}) than the corresponding vibrations in the water molecule (3400 cm^{-1}). Consideration of the corresponding zero point energies in the above equation for both H_2O and D_2O then leads to the expectation that the degree of dissociation should be greater in the former.

In the case of HSA, examination of the crystal structure in Fig. 1 suggests the dissolution is likely to involve the breaking up of the dimer units present in the surface. The magnitude of the kinetic isotope effect suggests that this may likely occur with proton dissociation. Either proton loss may irreversibly trigger solubilisation of the HSA unit, or, alternatively, a pre-equilibrium involving proton dissociation–reassociation could be envisaged. The latter would imply the exchangeability of the protons in the dimer hydrogen bonds with H_2O or D_2O in solution whereas in the former case the dissolution reaction would be:

$$1/2(HSA)_2(s) \rightarrow H^+(aq) + SA^-(s) \rightarrow H^+(aq) + SA^-(aq)$$

In conclusion, the kinetic solution isotope effects seen for the dissolution of solid salicylic acid suggest ionization of HSA prior to dissolution.

Notes and references

1 E. Hill and R. G. Compton, *Res. Chem. Kinet.*, 1997, **4**, 203.
2 J. V. MacPherson and P. R. Unwin, *Anal. Chem.*, 2001, **73**, 550.
3 G. H. W. Sanders, J. Booth and R. G. Compton, *Langmuir*, 1997, **13**, 3080.
4 B. A. Coles, R. G. Compton, J. Booth, Q. Hong and G. H. W. Sanders, *Chem. Commun.*, 1997, 619.
5 B. A. Coles, R. G. Compton, M. Suarez, J. Booth, Q. Hong and G. H. W. Sanders, *Langmuir*, 1998, **14**, 218.
6 S. J. Wilkins, M. Suarez, Q. Hong, B. A. Coles, R. G. Compton, G. E. Tranter and D. Firmin, *J. Phys. Chem. B*, 2000, **104**, 1539.
7 Thermomicroscopes Ltd., Bicester, Oxon, UK (http://www.thermomicroscopes.com).
8 Fluent Europe Ltd., Sheffield, UK (http://www.fluent.com).
9 S. J. Wilkins, B. A. Coles and R. G. Compton, *J. Phys. Chem. B*, in press.
10 L. Melander and W. H. Sanders, *Reaction Rates of Isotopic Molecules*, J. Wiley & Sons, New York, 1980, p. 214.
11 E. Fukuoka, M. Makita and S. Yamamuru, *Chem. Pharm. Bull.*, 1993, **41**, 1284.
12 ftp://joule.pcl.ox.ac.uk/pub/rgc/afmvmaps/. See ESI†.
13 M. M. Lobo, *Handbook of Electrolyte Solutions*, Elsevier, Oxford, UK, 1989.
14 W. E. Karsten, C. J. Lai and P. F. Cook, *J. Am. Chem. Soc.*, 1995, **117**, 5914.
15 B. A. Coles and R. G. Compton, http://physchem.ox.ac.uk/~rgc/research/afm/afm2.htm. See ESI†.
16 R. P. Bell, *Acids and Bases: Their Qualitative Behaviour*, Metheun & Co. Ltd., London, UK, 1971, p. 92.